10-17-2014

Geoacoustic Inversion of Ship Radiated Noise in Shallow Water Using Data from a Single Hydrophone

Steven E. Crocker
University of Rhode Island, steven.e.crocker@gmail.com

Peter L. Nielsen

James H. Miller
University of Rhode Island, miller@uri.edu

Martin Siderius

Citation/Publisher Attribution

Crocker SE, Nielsen PL, Miller JH, Siderius M. (2014). "Geoacoustic inversion of ship radiated noise in shallow water using data from a single hydrophone." JASA Express Letters. 136, EL362.
Available at: http://dx.doi.org/10.1121/1.4898739

Geoacoustic Inversion of Ship Radiated Noise in Shallow Water Using Data from a Single Hydrophone

Geoacoustic inversion of ship radiated noise in shallow water using data from a single hydrophone

Steven E. Crocker[a)]
Sensors and Sonar Systems Department, Naval Undersea Warfare Center, 1176 Howell Street, Newport, Rhode Island 02841
steven.crocker@navy.mil

Peter L. Nielsen
Centre for Maritime Research and Experimentation, viale San Bartolomeo, La Spezia, 19126, Liguria, Italy
nielsen@cmre.nato.int

James H. Miller
Department of Ocean Engineering, University of Rhode Island, 15 Receiving Road, Narragansett, Rhode Island 02882
miller@egr.uri.edu

Martin Siderius
Electrical and Computer Engineering, Portland State University, 1900 SW 4th Avenue, Portland, Oregon 97201
siderius@pdx.edu

Abstract: The Centre for Maritime Research and Experimentation conducted a geoacoustic inverse experiment in the Mediterranean Sea in the summer of 2012. Among the objectives was to employ an autonomous underwater vehicle to collect acoustic data to invert for properties of the seafloor. Inversion results for the compression wave speed in the bottom and the source spectrum of the *R/V Alliance* during a close approach to the bottom moored vehicle are presented. The estimated wave speed was 1529 m/s ($\sigma = 10$). The source spectrum of the *Alliance* was estimated across more than six octaves of frequency.

PACS numbers: 43.28.We, 43.30.Pc [WS]
Date Received: March 14, 2014 **Date Accepted:** October 8, 2014

1. Introduction

The objective of the inverse problem presented here was to simultaneously estimate properties of the acoustic source and the environment, using data collected by a single hydrophone. The acoustic source spectrum of a surface ship passing near a bottom moored autonomous underwater vehicle (AUV) was estimated across 19 contiguous 1/3 octave bands spanning more than 6 octaves of frequency. In addition, the compression wave speed and attenuation in marine sediments were estimated, where the bottom was parameterized as a fluid acoustic half-space with attenuation, for a total of 21 unknown parameters. Data subjected to inversion included geolocation information for the source and receiver, water depth, local sound speed profile, and acoustic pressure observed by the receiver hydrophone. Parameter estimates were calculated using a forward model based on the passive sonar equation and an objective function that was minimized using an evolutionary algorithm. Whereas characterization of the acoustic waveguide is the central objective of most geoacoustic inverse problems, the approach

[a)]Author to whom correspondence should be addressed.

described here also sought to estimate the power spectrum radiated by a passing ship by including the influence of the shallow water waveguide on signal attenuation.

2. Experiment

Data for this study were collected during the Glider Acoustic Sensing of Sediments 2012 (GLASS'12) experiment conducted in the Mediterranean Sea at the location shown in Fig. 1. The acoustic acquisition system included the acoustic array, signal conditioning, digital recording, and data storage integrated into a mission module that was installed in the vehicle. The system collected 8 channels of digital data at 100 kHz with 24-bit precision from an array with vertical and tetrahedral apertures mounted to the nose of the vehicle. Results reported here were based on analysis of data from a single hydrophone channel.

Ship radiated noise data were collected during a close pass of the *Alliance* [see Fig. 1(b)], with the AUV bottom moored in 18.5 m of water using a purpose built test stand that maintained the vehicle about 1.5 m above the seafloor. The water column was characterized by a typical downward refracting summer sound speed profile as illustrated in Fig. 2(a). The data set used for the inversion began with the closest point of approach (CPA) and extended for less than 2 min as the *Alliance* proceeded south at 5 m/s. Figure 2(b) illustrates received level (RL) data in the 250 Hz band during this event. (Also shown is the output of the forward model using parameter estimates generated by the inversion as will be discussed in Sec. 4.) Acoustic data representing the ambient and self-noise spectrum observed when the *Alliance* was loitering at a distance of 4 km were also used [see Fig. 2(c)]. The elevated noise levels in the 200 and 400 Hz bands were due to the power supply used for the hydrophone array.

Received acoustic band levels were estimated from data records that were 5 s in length with adjacent records overlapping by 50%. Each 5 s observation was decomposed into an ensemble of short buffers (e.g., 0.328 s) from which acoustic power spectra were computed. Received power spectra ($\Delta f \sim 3$ Hz) were integrated across the standard 1/3 octave bands ranging from 125 Hz to 8.0 kHz. Nine frequency bins were used to compute the 125 Hz band level. Other band levels were computed from commensurately larger numbers of frequency bins. Use of proportional band levels provided elements of the data vector with more uniform acoustic power in regions where the spectrum level varied inversely with frequency, as confirmed by inspection of the ambient noise spectrum of Fig. 2(c).

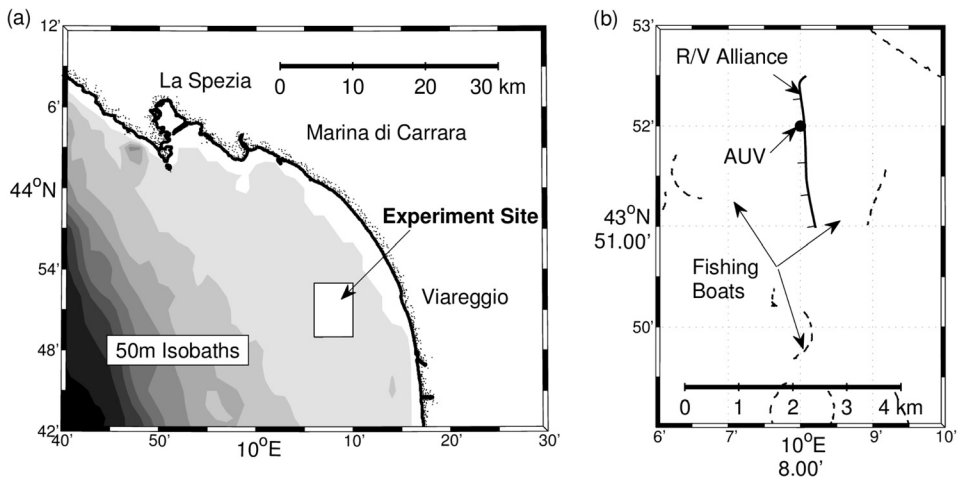

Fig. 1. GLASS'12 experiment site (a) approximately 10 km off the Italian coast near Viareggio, and (b) during a close pass by the *R/V Alliance*. Tick marks on ship's track provided at 2 min intervals.

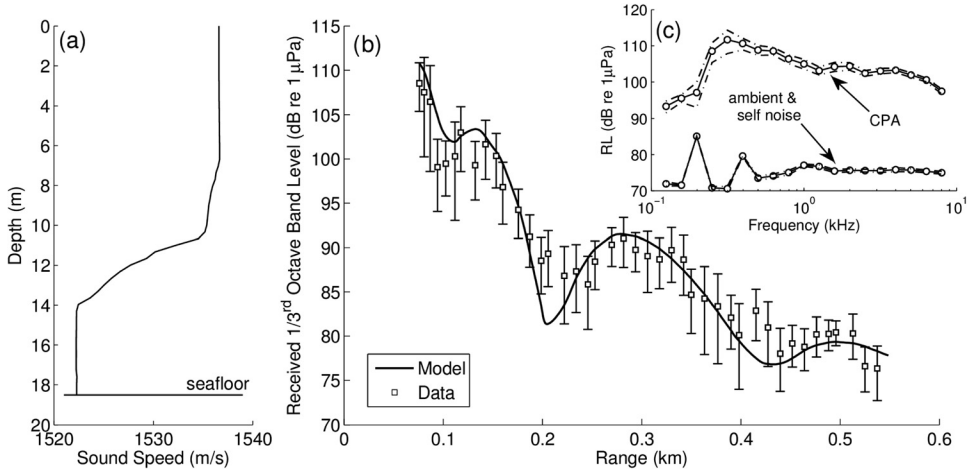

Fig. 2. GLASS'12 sea trial data: (a) Sound speed profile, (b) RL in 250 Hz 1/3 octave band including forward model result for reported parameter estimates, and (c) RL observed at CPA. Error bars delineate the interquartile range of acoustic observations.

Due to a moderately active population of shrimp, the median value of each 1/3 octave band level was used as the best estimate, the median being a more robust estimator than the mean when contending with noise from individual snapping shrimp. The spread of each observation was represented by the interquartile range, a measure of the statistical dispersion equal to the difference between the upper and lower quartiles. Thus, the inversion data were comprised of the location of the AUV, the *Alliance* track [Fig. 1(b)], the local sound speed profile [Fig. 2(a)], the noise radiated by *Alliance* as range from the AUV increased from 75 to 550 m [Fig. 2(b)], and the ambient noise observed in the absence of the *Alliance* [Fig. 2(c)].

3. Inversion method

3.1 Forward model

The inverse method developed for this study treated the acoustic source, the *Alliance*, as an unknown subject of the parameter estimation problem, in addition to certain properties of the seabed sediments. The acoustic source was modeled as a point source located at a depth of 3 m, corresponding to the propeller depth. A forward model predicted the received acoustic pressure in 1/3 octave band levels as a function of the unknown source spectrum, the ambient noise spectrum and the sediment, represented by an acoustic half-space.

An acoustic half-space parameterization was selected as a useful approximation of the seafloor despite the potential for significant variations in penetration depth across the inversion bandwidth. While the inversion bandwidth spanned more than 6 octaves, ship radiated acoustic power decreased sharply in frequency bands below 250 Hz as shown in Fig. 2(c). As a result, the signal observed in these bands faded quickly beneath the ambient noise floor as range to the *Alliance* increased, limiting the useful information available at the lowest frequencies and greatest penetration depths. In addition, geophysical data collected at the site were largely consistent with the simplified parameterization including two cores of 1 m depth and a sub-bottom profile that confirmed the absence of strong reflectors in the first several meters of the seafloor sediments.[1] Thus, sediment property estimates represent an average value in the first few meters beneath the seafloor, where available geophysical data confirmed the absence of strong inhomogeneity.

The sound speed profile, source-receiver positions, and sediment density were known quantities, the latter from the geophysical core data. Thus, the forward model

for the acoustic pressure amplitude P_o observed at frequency f was represented by the *Alliance* source spectrum P_s convolved with the magnitude of the acoustic transfer function H between the source and receiver separated by the horizontal distance r, together with the combined ambient and self-noise pressure amplitude P_a,

$$P_o^2(f, r) = P_s^2(f)\, H^2(f, r, c_b, a_b) + P_a^2(f), \tag{1}$$

where the compression wave speed and attenuation coefficient in the acoustic half-space were c_b and a_b, respectively. Dependence of the acoustic transfer function H on sediment density and sound speed profile in the water is implicitly assumed in Eq. (1). Frequency dependent, acoustic transfer functions were computed using the normal mode model KrakenC (Ref. 2) with the upper phase speed limit set to 10^5 m/s to account for propagation over shorter ranges and steeper angles. The magnitudes of the acoustic transfer functions were estimated as the average value for ten discrete frequencies linearly distributed over each 1/3 octave band.

3.2 Nonlinear optimization

An objective function was defined to guide the directed search for the set of model parameters that best explained the observed data. The data on which the objective function operated were the acoustic pressure amplitudes in contiguous 1/3 octave bands ranging from 125 Hz to 8.0 kHz observed at 42 source-receiver separations between 75 and 550 m for a total of $N = 798$ observations. The error associated with the nth frequency-distance pair in the $[N \times 1]$ error vector $\mathbf{e}$ was

$$\mathrm{e}(n, \mathbf{m}) = \ln\left(\frac{P_m(n, \mathbf{m})}{P_o(n)}\right), \tag{2}$$

where P_m was the acoustic pressure predicted by the forward model for parameter set $\mathbf{m}$. An objective function based on this error vector was defined as

$$\phi(\mathbf{m}) = ((\mathbf{w} \cdot \mathbf{e}(\mathbf{m}))^T (\mathbf{w} \cdot \mathbf{e}(\mathbf{m})))^{1/2}, \tag{3}$$

with T the transpose operator. The weight vector $\mathbf{w}$ was used to provide observations with greater statistical spread with proportionally less influence over the objective function value. In particular, each observation was weighted by the inverse of its interquartile range such that

$$\mathbf{w} = \frac{N}{\sum_{n=1}^{N} \frac{P_{on}}{q_n}} \left[\frac{P_{o1}}{q_1}, \frac{P_{o2}}{q_2}, \frac{P_{o3}}{q_3}, \ldots, \frac{P_{oN}}{q_N}\right]^T, \tag{4}$$

where q_n was the interquartile range of the nth observation. Thus, the inverse problem was reduced to a directed search for the set of model parameters $\mathbf{m}$ that minimized the difference between the acoustic observations P_o and the prediction of the forward model $P_m(\mathbf{m})$ as measured by the objective function $\phi(\mathbf{m})$.

A global search strategy based on the differential evolution[3] algorithm was used to minimize Eq. (3). The optimization was initialized with a population comprised of 10 individuals for each unknown parameter for a total of 210 members. The optimization was started with the initial population randomly (uniform) distributed throughout the bounded parameter search space $\mathbf{M}$. Source level bounds were centered on the spectrum observed at CPA plus an estimate for the transmission loss in a spherically divergent wave field. The upper and lower bounds spanned ± 20 dB about this reference value, plus an additional factor for the interquartile range of data observed at CPA. Parameter bounds for sound speed in the bottom were 1000 to 2000 m/s. The

attenuation coefficient a was bounded at 0 to 1, where the frequency dependent attenuation α was modeled as

$$\alpha = \frac{af}{10^3} \text{ dB/m}, \tag{5}$$

with f the frequency in Hz.

3.3 Parameter value and uncertainty estimates

Parameter values and their uncertainties were expressed using *a posteriori* probability distributions derived from a maximum likelihood approach[4] where the *a priori* U and *a posteriori* G probability distributions were related through a likelihood function L as

$$G(\mathbf{m}) = L(\mathbf{m})\, U(\mathbf{m}), \tag{6}$$

and the one-dimensional marginal *a posteriori* probability density function for the ith parameter $G_i(m_i)$ was the integral of the M dimensional probability density with respect to all parameters m_j for $j = 1, 2, ..., M$ and $i \neq j$ to yield

$$G_i(m_i) = \int \cdots \int G(\mathbf{m})\, dm_1 \cdots dm_{i-1}\, dm_{i+1} \cdots dm_M. \tag{7}$$

Numerical methods to estimate the integrals of Eq. (7) include importance sampling where the integrand is non-uniformly sampled to concentrate the computational effort to regions that contribute most to the integral. The differential evolution algorithm implements importance sampling using a generating distribution to select the trial model vectors. While the generating distribution is unknown and evolves over the course of the optimization, a large number of candidate solutions are generated from the model parameter space $\mathbf{M}$. As a result, the model vectors $\mathbf{m}$ and objective function values ϕ computed during the optimization process can be used to estimate the integrals of Eq. (7).[5]

An estimate for the *a posteriori* probability of the kth model vector based on the N_p model vectors in the population at the conclusion of the optimization process is

$$\hat{G}(\mathbf{m}_k) = \frac{L(\mathbf{m}_k)\, U(\mathbf{m}_k)}{\sum_{j=1}^{N_p} L(\mathbf{m}_j)\, U(\mathbf{m}_j)}, \tag{8}$$

with the *a priori* probabilities U uniformly distributed between the bounds defined for each element in the model parameter vector $\mathbf{m}$. Thus, estimation of the *a posteriori* probabilities was effectively maximum likelihood within defined parameter bounds.

The marginal probability distribution for obtaining the particular value K for the ith parameter m_i in the model vector is

$$\hat{G}_i(K) = \sum_{k=1}^{N_p} \hat{G}(\mathbf{m}_k)\, \delta(m_{k,i} - K). \tag{9}$$

Since the likelihood function L is usually related to the objective function $\phi(\mathbf{m})$ through an exponential, an empirical estimate of the likelihood function is

$$L(\mathbf{m}) = \exp\left(\frac{-(\phi(\mathbf{m}) - \phi(\mathbf{m}_o))}{T}\right), \tag{10}$$

where $\mathbf{m}_o$ is the estimated parameter vector for the optimum value of the objective function and T is a constant that is particular to each optimization. The parameter T

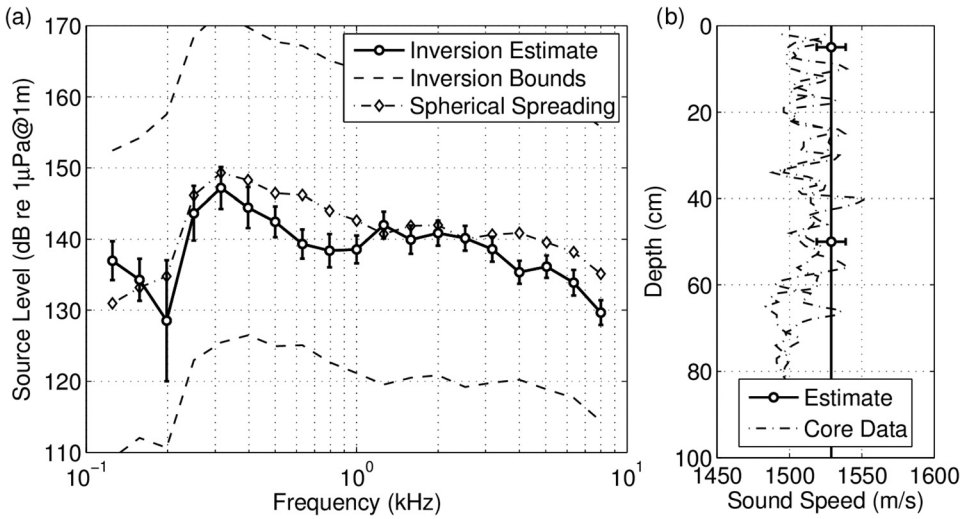

Fig. 3. GLASS'12 inversion results (a) *R/V Alliance* source spectrum estimate, and (b) sediment compression wave speed. Parameter estimates presented as the mean plus and minus one standard deviation ($\mu \pm \sigma$) for the *a posteriori* probability distributions.

was set to the average of the 50 best objective functions obtained during the optimization minus the best objective function value, a value that experience has shown to be a good choice,[6]

$$T = \frac{1}{50}\sum_{n=1}^{50} \phi(\mathbf{m}_n) - \phi(\mathbf{m}_o). \tag{11}$$

4. Result

Inversion results for the source spectrum and sediment compression wave speed are provided as Figs. 3(a) and 3(b), respectively. Parameter estimates are presented as the mean plus and minus one standard deviation ($\mu \pm \sigma$) for the marginal *a posteriori* probability distributions. The source spectrum estimate included the reference value determined by assuming a spherically divergent acoustic field between the *Alliance* and the bottom moored AUV while at CPA. The relatively large uncertainty in the source level estimated for the 200 Hz band ($\sigma = 8.5$ dB) was due to electronic noise in the data recording system [see Fig. 2(c)] and the correspondingly low signal-to-noise ratio in this band. The standard deviations of the estimated source level distributions were otherwise on the order of two to three decibels.

The estimated compression wave speed is illustrated in Fig. 3(b), where the bottom was modeled as a homogeneous, acoustic half-space. Also shown in the figure are the compression wave speeds measured in 2 cores taken within 500 m of each other and the AUV deployment location. The compression wave speed estimate of 1529 m/s ($\sigma = 10$) agrees well with the mean value of 1510 m/s ($\sigma = 15$) that was measured in the cores. The inversion did not converge on an estimate for attenuation in the sediment; its influence on the value of the objective function being negligible as verified by a marginal sensitivity analysis performed using a synthetic data set. In short, the transmission path length was insufficient (e.g., ~30 water depths) to accumulate a detectable level of attenuation due to absorption as consideration of Eq. (5) suggests. Finally, Fig. 2(b) provides a comparison of the RLs observed in the 250 Hz band to those calculated by the forward model (KrakenC) using the set of model parameters estimated by the inversion, where good agreement was found.

5. Conclusion

Acoustic data collected by a hydrophone mounted to a bottom moored AUV were successfully inverted for the broadband source spectrum of a passing ship and the compression wave speed in the seafloor sediments. Formulation of the inverse problem was atypical in that it cast *Alliance's* source level in each of the 1/3 octave bands as independent and unknown parameters subject to estimation simultaneously with the compression wave speed in the sediment. A maximum likelihood approach was used to estimate the *a posteriori* probability distributions for each of the model parameters. The standard deviations associated with these probability distributions were presented where good agreement was found between the measured and estimated compression wave speed. Inverse problems of this type are not only of interest where the use of a ship of opportunity is concerned, but also when an estimate of the acoustic source spectrum radiated by that ship is desired.

Acknowledgments

The authors would like to thank the personnel of the CMRE Engineering Department for their development of the acoustic array deployed on the AUV and for their support during the sea trial. The authors are also grateful for the professionalism of the officers and crew of the *R/V Alliance*. This work was supported by CMRE, the Office of Naval Research, and the Underwater Sound Reference Division at the Naval Undersea Warfare Center.

References and links

[1]P. L. Nielsen, M. Siderius, J. Miller, S. Crocker, and J. Giard, "Seabed characterization using ambient noise and compact arrays on an autonomous underwater vehicle," Proc. Meet. Acoust. **19**(1), 070030 (2013).

[2]M. B. Porter, "The KRAKEN normal mode program," Technical Report, Naval Research Laboratory (1992).

[3]R. M. Storn and K. V. Price, "Differential evolution—a simple and efficient heuristic for global optimization over continuous spaces," J. Global Optim. **11**(4), 341–359 (1997).

[4]P. Gerstoft and C. F. Mecklenbräuker, "Ocean acoustic inversion with estimation of *a posteriori* probability distributions," J. Acoust. Soc. Am. **104**(2), 808–819 (1998).

[5]S. E. Crocker, J. H. Miller, G. R. Potty, J. C. Osler, and P. C. Hines, "Nonlinear inversion of acoustic scalar and vector field transfer functions," IEEE J. Ocean. Eng. **37**(4), 589–606 (2012).

[6]P. Gerstoft and D. G. Gingras, "Parameter estimation using multifrequency range–-dependent acoustic data in shallow water," J. Acoust. Soc. Am. **99**(5), 2839–2850 (1996).